HHS Public Access

Author manuscript

Cell. Author manuscript; available in PMC 2016 November 05.

Published in final edited form as:

Cell. 2015 November 5; 163(4): 907–919. doi:10.1016/j.cell.2015.10.022.

Vesicle-Mediated Steroid Hormone Secretion in *Drosophila melanogaster*

Naoki Yamanaka[1,2,*], **Guillermo Marqués**[3], and **Michael B. O'Connor**[1,*]

[1]Department of Genetics, Cell Biology and Development, University of Minnesota, Minneapolis, MN 55455, USA

[2]Department of Entomology, Institute for Integrative Genome Biology, Center for Disease Vector Research, University of California, Riverside, Riverside, CA 92521, USA

[3]University Imaging Centers, University of Minnesota, Minneapolis, MN 55455, USA

SUMMARY

Steroid hormones are a large family of cholesterol derivatives regulating development and physiology in both the animal and plant kingdoms, but little is known concerning mechanisms of their secretion from steroidogenic tissues. Here we present evidence, that in *Drosophila*, endocrine release of the steroid hormone ecdysone is mediated through a regulated vesicular trafficking mechanism. Inhibition of calcium signaling in the steroidogenic prothoracic gland results in the accumulation of unreleased ecdysone, and the knockdown of calcium-mediated vesicle exocytosis components in the gland caused developmental defects due to deficiency of ecdysone. Accumulation of Synaptotagmin-labeled vesicles in the gland is observed when calcium signaling is disrupted, and these vesicles contain an ABC transporter that functions as an ecdysone pump to fill vesicles. We propose that trafficking of steroid hormones out of endocrine cells is not always through a simple diffusion mechanism as presently thought, but instead can involve a regulated vesicle-mediated release process.

INTRODUCTION

Steroid hormones are an important class of bioactive molecules in both animal and plant kingdoms that regulate a wide variety of physiological processes including immune response, salt and water balance, glucose metabolism, and sexual maturation during juvenile development (Sapolsky et al., 2000; Sisk and Foster, 2004). In insect larvae, the primary precursor steroid hormone ecdysone (E) is produced in the prothoracic gland (PG). After its release into the circulatory system, E is taken up in peripheral tissues such as the gut and fat

*Correspondence: naoki.yamanaka@ucr.edu (N.Y); moconnor@umn.edu (M.B.O).

AUTHOR CONTRIBUTIONS

N.Y. and M.B.O. conceived the research; G.M. performed GCaMP5 imaging; N.Y. performed all the other experiments; N.Y., G.M. and M.B.O. analyzed the data; N.Y. and M.B.O. wrote the manuscript.

body where it is converted to 20-hydroxyecdysone (20E). This is the active derivative that regulates larval molt timing and the onset of metamorphosis leading to the formation of sexually mature adults (Yamanaka et al., 2013a).

The biosynthetic pathways of steroid hormone production have been extensively studied in diverse animal species, and many of the key enzymes have been identified and well characterized (Ghayee and Auchus, 2007; Huang et al., 2008; Miller, 2013). In insects, E biosynthesis is stimulated by extracellular signaling molecules such as the prothoracicotropic hormone (PTTH), which binds to its receptor Torso to induce the expression of genes encoding steroidogenic enzymes (Rewitz et al., 2009; Yamanaka et al., 2013a).

In contrast to the extensive literature describing studies on steroidogenic processes, very little is known about the mechanisms that regulate release of steroid hormones from endocrine tissues. Indeed, the textbook view is that lipophilic steroid hormones simply enter and exit cells by diffusion across lipid bilayers (Raven and Johnson, 2002; Sherwood, 2011; White and Porterfield, 2012). However, this prevailing assumption has not been extensively tested *in vivo*, and the limited studies described so far primarily used *in vitro* or *in silico* approaches (Oren et al., 2004; Watanabe et al., 1991).

Given the scarcity of knowledge concerning this fundamental aspect of endocrinology, we used molecular genetic tools to investigate the mechanism of E release from the PG in *Drosophila melanogaster*. We found that blocking calcium signaling through RNAi-mediated knockdown of the *inositol 1,4,5,-trisphosphate receptor* (*IP3R*) in the PG leads to a buildup of E and a decrease of 20E in source and target tissues, respectively. This results in severe delay or larval developmental arrest that can be rescued by feeding larvae E. Identical developmental defects were observed in larvae in which cellular components normally involved in calcium-mediated vesicle exocytosis, such as Rab3, UNC-13 or Synaptotagmin 1 (Syt1), were depleted in the PG. Moreover, GCaMP imagining of the PG just prior to metamorphosis revealed spontaneous calcium signaling that was attenuated by RNAi-mediated knockdown of the upstream signaling component that couples G protein-coupled receptors (GPCRs) to calcium release. Furthermore, the accumulation of Syt1-positive vesicles was observed when calcium signaling was blocked in the PG, suggesting that calcium-mediated vesicle exocytosis is required for E release. Consistent with this notion, we identified an ABC transporter found in these Syt1-positive vesicles and show that it transports E across a lipid bilayer *in vitro*. Taken together, these results support a new hypothesis that transport of steroid hormones across lipid bilayers can involve a regulated vesicle-release process instead of, or in addition to, passive or facilitated diffusion mechanisms.

RESULTS

IP3R-Mediated Calcium Signaling Is Required for E Secretion from the PG

Studies using isolated PGs of lepidopteran insect species have long suggested a key role for calcium in stimulating E production and release in response to PTTH (Huang et al., 2008). To test this in *Drosophila*, we conducted PG-specific knockdown of *IP3R*, which encodes an

intracellular calcium-release channel. *IP3R* is highly expressed in the PG and mutants have growth defects due to low systemic levels of E (Venkatesh and Hasan, 1997), but direct links between the IP3R function and E production or release have yet to be tested. When *IP3R* RNAi was induced using the PG driver *phm22-Gal4*, we observed polyphasic growth arrest throughout larval development (Figure 1A). Those larvae that arrested in the third instar stage showed an overgrowth phenotype due to an extended larval feeding period, which is commonly observed for E-deficient animals (Figure 1B) (Caceres et al., 2011; Ou et al., 2011; Rewitz et al., 2009; Talamillo et al., 2008). Feeding E to these larvae rescued the arrest phenotype, further suggesting that the systemic E level is low in these animals. Even those individuals that eventually initiated metamorphosis (~60%) only did so after a significant delay (Figure 1C) and also exhibited an overgrowth phenotype (Figure 1D), both of which were fully rescued by E feeding. Importantly, however, neither the larval arrest nor pupariation delay phenotype was fully rescued by overexpressing Ras^{V12}, the active form of Ras that is able to completely rescue a PTTH signaling deficiency (Figures 1A and 1C) (Rewitz et al., 2009). Such partial rescue strongly suggests that, unlike previous assumptions based on moth studies (Huang et al., 2008), the intracellular calcium release mediated by IP3R is not solely functioning upstream of the MAPK signaling cascade and E synthesis, but is likely regulating other processes in the *Drosophila* PG.

One hypothesis we considered was that calcium signaling might play a role in E release from the PG as opposed to, or in addition to, E synthesis. As a first test of this hypothesis, we sought to quantify E and 20E in the PG of *phm22>IP3R RNAi, dicer2* larvae. The PG is part of a composite endocrine organ called the ring gland (RG), which is attached to the central nervous system (CNS). The small size of the RG presents a substantial dissection challenge. Therefore, we dissected the larger CNS-RG complex, extracted steroids with methanol, and separated E from 20E by high-performance liquid chromatography (HPLC). The E and 20E containing fractions were quantified using an enzyme-linked immunosorbent assay (ELISA) for ecdysteroids (Figure 1E). This analysis revealed that the titers of both E and 20E increase in the CNS-RG complex of control larvae during the wandering stage as they prepare for metamorphosis (Figure 1F). This observation is consistent with the notion that the E biosynthetic activity of the PG is stimulated by PTTH during this period and the increased levels of 20E in the hemolymph help initiate wandering behavior when taken up by the brain (Yamanaka et al., 2013b). In control larvae, the titer of 20E was substantially higher than that of E in the CNS-RG complex during the wandering stage, indicating that the release of E into the hemolymph and its conversion to 20E happens quickly under normal conditions. Indeed, the 20E titer in the hemolymph increased rapidly in wandering control larvae, while the E titer remained constant or decreased during this stage (Figure 1G). In the case of *phm22>IP3R RNAi, dicer2* larvae, however, the ecdysteroid composition in the CNS-RG complex was markedly different; the E titer was elevated above that seen at any stage in control larvae, and the titer of 20E was less instead of more than E (Figure 1F). For *IP3R*-knockdown animals that are developmentally delayed, we used wandering as a behavioral trait and used 150 h after egg laying (AEL) wandering larvae for hormone titer measurement, in order to ensure that we are examining hormone titers at the same developmental stage. Consistent with this notion, the hemolymph levels of ecdysteroids in these *IP3R*-knockdown animals were comparable to those of early wandering control

animals (Figure 1G). From these results, we infer that: 1) E is still produced in the PG even when the intracellular calcium release is down-regulated by *IP3R RNAi*, and 2) the release of E into the hemolymph is inhibited upon *IP3R* knockdown, resulting in the accumulation of E in the PG.

Components That Regulate Secretory Vesicle Exocytosis Are Required for Proper PG Function

The above results led us to hypothesize that E secretion from the PG is not a fully passive or facilitated diffusion process, but instead may employ a regulatory mechanism that is under the control of calcium signaling. This is reminiscent of secretory vesicle exocytosis in neurons and endocrine cells, where the fusion of vesicles containing neurotransmitters, or various types of hormones, with the plasma membrane is tightly regulated by multiple components that sense intracellular calcium concentrations (Rizo and Rosenmund, 2008; Sudhof, 2004). Therefore, we conducted RNAi knockdown screening of components known to be either upstream regulators of intracellular calcium release or downstream effectors of calcium-regulated secretory vesicle exocytosis (Table 1 and Figure 2A).

There are two distinct genes encoding intracellular calcium-release channels in *Drosophila*: *IP3R* and *Ryanodine receptor* (*RyR*) (Sorrentino et al., 2000). The knockdown of *IP3R* in the PG showed the larval arrest phenotype as described above, whereas that of *RyR* did not cause any discernible defect (Table 1). IP3R is activated by inositol 1,4,5,-tris-phosphate produced by phospholipase C (PLC) enzymes, which are encoded by three genes in *Drosophila* (Shortridge and McKay, 1995). PG-specific RNAi knockdown of one of them, *Plc21C*, caused the larval arrest phenotype (Table 1). *Plc21C* encodes a member of PLCβ class of enzymes, which are typically activated by the Gαq subunit of heterotrimeric G proteins coupled with GPCRs. Although RNAi-mediated knockdown of *Gaq* did not cause developmental arrest, we identified *CG30054* and *CG17760* as two adjacent genes that are highly homologous to *Gaq* (Figures S1A and S1B). PG-specific knockdown of *CG30054*, but not that of *CG17760*, caused a developmental defect similar to knockdown of *Plc21C* and *IP3R* (Table 1). Taken together, these results indicate that the calcium mobilization from intracellular stores through IP3R is regulated by GPCR(s) in the PG (Figure 2A), further suggesting that there is an as-yet-unknown signaling pathway acting in parallel with the PTTH/Torso/MAPK pathway to facilitate E release as opposed to its production.

The ternary SNARE complex that consists of synaptobrevin/VAMP, SNAP-25 and syntaxin plays a pivotal role in various types of vesicle exocytosis in eukaryotes ranging from yeast to human (Li and Chin, 2003; Richmond and Broadie, 2002; Rizo and Rosenmund, 2008; Sudhof, 2004). Indeed, the PG-specific knockdown of *Syb*, one of the two synaptobrevins in *Drosophila*, causes the larval arrest phenotype, supporting the hypothesis that calcium-regulated vesicle exocytosis is required for E secretion (Table 1). The SNARE complex, however, is involved in all intracellular membrane fusion events, and each organism has multiple SNARE proteins that are localized to distinct membrane compartments to specify intracellular compartmental identity (Li and Chin, 2003). These diverse SNARE complex functions make it difficult to interpret the above result, since E synthesis in the PG involves the trafficking of synthetic intermediates between organelles, and the disruption of this

process is expected to cause similar developmental defects. Likewise, the necessity of the exocyst complex components in the PG (Table 1 and Andrews et al., 2002) is difficult to attribute solely to its potential role in E secretion, since this complex is required for multiple membrane trafficking events, including the transport of vesicles carrying transmembrane receptors from the trans-Golgi network to the plasma membrane (Langevin et al., 2005; Murthy et al., 2003). That knockdown of exocyst complex members does disrupt trafficking of transmembrane proteins to the plasma membrane is clearly shown by the depletion of mCD8-GFP in the plasma membrane of PG cells of larvae expressing *phm22>Sec10 RNAi* (Figure S2). Such a defect will likely disrupt several signaling pathways including PTTH and insulin signaling, both of which require the transport of their receptors to the PG plasma membrane for high level E production (Yamanaka et al., 2013a).

In light of these difficulties in interpreting the phenotypes produced by knockdown of general secretory machinery subunits, we focused our analysis on components that are more specifically involved in calcium-regulated exocytosis. UNC-13 is a highly conserved, plasma membrane-associated presynaptic protein with calcium-binding domains. It interacts with the SNARE protein syntaxin and primes synaptic vesicles for fusion, and is essential for calcium-regulated synaptic vesicle exocytosis (Aravamudan et al., 1999; Richmond et al., 2001). There are three *Drosophila* genes that encode UNC-13 family proteins, and knockdown of only *CG34349* produced the larval arrest phenotype (Table 1 and Figure 2B). Likewise, one of the secretory Rab GTPases, Rab3, and its interacting molecule RIM, both of which are involved in secretory vesicle trafficking and priming (Fukuda, 2008; Graf et al., 2012; Muller et al., 2012), are also essential for proper function of PG cells (Table 1 and Figure 2). Synaptotagmins, which form another class of calcium sensor proteins critical for vesicle exocytosis (Chapman, 2008; de Wit et al., 2009), were also tested for their necessity in the PG, and only Syt1 was found to be required for PG function (Table 1 and Figure 2). The knockdown phenotypes of these regulatory exocytosis components were strikingly similar to that of *IP3R*; they all showed polyphasic larval developmental arrest and pupariation delay accompanied by overgrowth, both of which were rescued by E feeding (Figure 2). Moreover, unlike *Sec10* RNAi, the knockdown of these components in the PG did not disrupt the plasma membrane localization of the mCD8-GFP reporter, suggesting that constitutive membrane traffic is not altered (Figure S2).

To further validate that the calcium signaling pathway is active in the PG cells at the time of metamorphosis initiation, we monitored calcium dynamics in these cells using the genetically encoded calcium indicator, GCaMP5 (Akerboom et al., 2012). As illustrated in Figures 2D and 2E, two types of spontaneous activities were observed in the PG cells of wandering larvae. One consisted of major concentration changes throughout the entire volume of a PG cell, which we refer to as macro spikes (Figures 2D and 2E and Movie S1). The number of active cells within a gland varied significantly, and the dynamics of the calcium concentration observed also varied in amplitude, duration and frequency on a cell by cell basis (Figure 2E). A second activity, which we refer to as micro spikes (Figure 2E), appeared to occur in a limited area on the cell surface and exhibited faster kinetics. When the PG-specific knockdown of *Plc21C* was performed with two distinct RNAi constructs, a significant decrease in the number of animals exhibiting calcium dynamics of either class

was observed (Figure 2F), while RNAi of a random control gene (*gbb*) had no effect. These results support the notion that GPCR-mediated calcium signaling is occurring in the PG cells prior to metamorphosis.

In order to genetically validate the coupling of GPCR-regulated calcium release and vesicle exocytosis, an activated form of *Gαq* (*Gαq[Q203L]*) was expressed in the PG (Figure S1C). Interestingly, constitutive activation of Gαq pathway in the PG led to early larval lethality, suggesting that timely activation of GPCR signaling pathway is critical for proper larval development. Importantly, this early larval lethality was rescued by co-expressing RNAi constructs of the anticipated downstream components (*IP3R*, *CG34349*, *Rab3* and *Syt1*; Figure S1C) and more larvae developed into L3 or beyond, consistent with the knockdown phenotypes of those downstream genes (Figures 1 and 2). Taken together, these results suggest that the GPCR-regulated calcium release through IP3R is indeed coupled with vesicle exocytosis in the PG cells.

Syt1-positive Vesicles Accumulate in the PG upon Calcium Signaling Knockdown

In order to visualize putative secretory vesicles whose exocytosis is regulated by calcium signaling we expressed in the PG eGFP-tagged Syt1 (Syt-GFP), a widely used secretory vesicle marker in both neuronal and non-neuronal cells (Sugita et al., 2001; Zhang et al., 2002). In wildtype larvae, Syt-GFP labeled both the plasma membrane and a small number of vesicles in the PG (Figures 3A and 3C). It is known that Syt-GFP often labels the plasma membrane, depending on its expression level (Kanno and Fukuda, 2008). Interestingly, knocking down *IP3R* in the PG resulted in prominent accumulation of the Syt-GFP vesicles in the cytoplasm, especially in the areas adjacent to the plasma membrane (Figures 3B, 3D and 3E). *IP3R* knockdown in the PG did not alter the gross morphology of the PG (Figures 3B and S2), although the size of each cell might be slightly increased, which is potentially coupled with the accumulation of vesicles in the cytoplasm. This accumulation of Syt-GFP vesicles at the plasma membrane was typically observed in the PGs of *IP3R* RNAi larvae during the extended third instar stage (*i.e.* after 140 h AEL), at the time when E accumulation was observed in the CNS-RG complexes (Figure 1F). This observation is consistent with our hypothesis that E is loaded into Syt1-positive secretory vesicles in the PG and is released into the hemolymph via exocytosis triggered by calcium signaling.

Atet Is an ABC Transporter Present in Syt1-positive Vesicles in the PG

If E indeed requires vesicle-mediated machinery to be released from the PG, there should be transporters on the vesicle surface that load E into the vesicles. There is an ATP-binding cassette (ABC) transporter, E23, which has been proposed to function as a 20E exporter to modulate the effective intracellular concentration of 20E in peripheral tissues in *Drosophila* (Hock et al., 2000). E23 is a member of the ABCG subfamily of ABC transporters, several of which in mammals have been shown to help efflux cholesterol and other types of steroids such as estrogens and their metabolites (Imai et al., 2003; Janvilisri et al., 2003; Klucken et al., 2000; Suzuki et al., 2003; Wang et al., 2004; Yu et al., 2005). Based on these previous findings, an *in situ* hybridization screening of ABCG transporter genes in *Drosophila* genome (Figure S3) was conducted to identify putative E transporters highly expressed in the PG. This resulted in the identification of *Atet* and *CG4822*, both of which are highly

expressed in the PG of third instar larvae (Figures 4A and S3). Of these two genes, only knockdown of *Atet* in the PG showed developmental defects indistinguishable from those of knockdown of calcium-regulated vesicle exocytosis genes (Figures 4B–D) and were also rescued by E feeding.

We next expressed a fluorescent protein-tagged Atet in the PG to visualize its subcellular localization. This resulted in the labeling of both the plasma membrane and Syt1-positive vesicles (Figure 4E), suggesting that Atet could indeed be involved in the import of E into these vesicles. The signal of fluorescent protein-tagged CG4822, in contrast, did not co-localize with that of Atet in the PG (Figure S3E).

Atet Transports E across Membranes *in vitro* in an ATP-Dependent Manner

In order to further examine if Atet is a critical transporter for loading E into PG secretory vesicles, we sought to develop an *in vitro* transport assay. We first analyzed the predicted membrane topology of Atet using Phobius, a transmembrane protein topology and signal peptide predictor program (Kall et al., 2007). To our surprise, Atet was predicted to have an extracellular N-terminus, despite the fact that its ATP binding domain is on its N-terminal side (Figure 5A). The same result was obtained using two other independent algorithms (TMHMM version 2.0 (Krogh et al., 2001) and HMMTOP version 2.0 (Tusnady and Simon, 2001)), although the number of transmembrane domains differed between prediction algorithms. To determine the actual topology of Atet, we expressed an N-terminally HA-tagged Atet in Schneider 2 (S2) cells, a cell line derived from a primary culture of late stage *Drosophila* embryos, and immuno-stained the cells in both permeabilized and non-permeabilized conditions (Figure 5B). Under permeable conditions, both the surface of the cells and the internal structures were stained, suggesting that a certain population of Atet proteins are localized on the plasma membrane as in the PG cells. Importantly, under non-permeable conditions, N-terminal staining of Atet was still detected on the surface of the cells, whereas the control E23 tagged at the intracellular C-terminus was not detected without permeabilizing the cells (Figure 5B). These observations demonstrate that the N-terminus of Atet is indeed located on the non-cytoplasmic side of the membranes.

Based on this atypical membrane topology of Atet, we designed an *in vitro* transport assay using S2 cell membrane vesicle preparations from cells transfected with Atet (Figure S4). A crude membrane preparation typically contains both inside-out and right-side-out vesicles. In a regular vesicular ABC transporter assay, only the activity of the transporters in the inside-out vesicle configuration are detected, since a typical ABC transporter in the right-side-out vesicles will have its ABC domain inside the vesicles and therefore unable to access the exogenously added ATP and transport substrate. Thus, activity is measured as the amount of substrate imported into the vesicles (Figure S4). In contrast, in the case of Atet, no net flux into vesicles would be expected upon addition of exogenous substrates since Atet is predicted to pump substrates in the opposite direction. Therefore, in our modified procedure, the substrate E was preloaded into vesicles during isolation and then ATP was added to assess the transporter activity as efflux rather than influx. (Figure S4). As shown in Figure 5C, addition of ATP significantly stimulated efflux of E from Atet containing vesicles while no transport was observed using E23, a putative E transporter with a ‘normal’

membrane configuration with respect to the ABC domain. These results demonstrate that Atet can indeed transport E from the cytoplasmic to non-cytoplasmic side of vesicle membranes, providing strong support for our vesicle-mediated E release model (Figure 6).

DISCUSSION

In the present study, we provide several lines of evidence demonstrating that the insect steroid hormone E is secreted from the PG not by simple diffusion, but rather through a calcium signaling-regulated vesicle fusion event. Below we discuss three major points of our findings: 1) Atet, an ABCG transporter, can facilitate E passage through membranes in an ATP-dependent manner, 2) GPCR-regulated calcium signaling in the PG promotes E release, and 3) the significance of steroid hormone release by vesicle exocytosis and its implication for other steroid hormone/cholesterol trafficking processes.

The ABCG Family Member Atet Is an E Transporter

Atet was originally cloned in *Drosophila* as an ABC transporter-encoding gene with unknown function. It was found to be highly expressed in embryonic trachea, leading to its name *ABC transporter expressed in trachea* or *Atet* (Kuwana et al., 1996). In our *in situ* hybridization experiment, however, we found little expression of *Atet* in embryonic trachea, but instead saw specific high level expression in the PG (Figure S3F), consistent with its expression pattern in the third instar larva (Figure 4A). Since we found that Atet has an atypical membrane topology (Figures 5A and 5B) and can transport E across membranes *in vitro* (Figure 5C), we propose renaming this gene *Atypical topology ecdysone transporter*, thereby retaining the *Atet* gene designation.

Atet belongs to the ABCG subfamily of ABC transporters, members of which in mammals have been shown to transport cholesterol as well as other steroids, such as estrogens and their metabolites, in many biological systems (Imai et al., 2003; Janvilisri et al., 2003; Klucken et al., 2000; Suzuki et al., 2003; Wang et al., 2004; Yu et al., 2005). To our knowledge, however, the atypical membrane topology, with the N-terminal ABC domain on the non-cytoplasmic side of the membrane, has not been reported for any ABC transporter to date. However, this topology may have a strong advantage in facilitating tight control on E release by preventing Atet from functioning on the plasma membrane, due to the lack of ATP in extracellular space. This configuration therefore prevents E transport directly through the plasma membrane and confines it to a vesicle mediated fusion process, although it requires a separate molecular mechanism to transport ATP into the secretory vesicles. This mechanism remains unclear at this point, but it may involve a specific transporter like the recently described VNUT/SLC17A9 (Sawada et al., 2008). In this context, it is interesting to note that the human Atet orthologs ABCG1 and ABCG4 (Figure S3A) are also strongly predicted by membrane topology algorithms to position their N-terminal ABC domain on the non-cytoplasmic side. These transporters mediate cellular cholesterol efflux (Wang et al., 2004) and have recently been shown to work not on the plasma membrane but in intracellular endosomes (Tarling and Edwards, 2011). Clearly, additional studies on the membrane topology of ABCG transporters are warranted.

Separate Signaling Pathways Likely Regulate E Production and Release

The results of our RNAi screening (Table 1) demonstrate that CG30054, a Gαq subunit, and Plc21C, a PLCβ class enzyme, are both required for proper PG function. These findings strongly implicate the existence of an unknown GPCR and cognate ligand as mediators of the calcium signaling event that we suggest stimulates E release from the PG. On the other hand, we know that the PTTH receptor is Torso, a receptor tyrosine kinase (Rewitz et al., 2009) and its primary role is to promote E production by inducing E biosynthetic enzyme gene transcription. These observations suggest that, at least in *Drosophila*, E production and release are likely regulated separately. This machinery might help the GPCR ligand to generate large pulses of steroid in a timely fashion. The identification of the GPCR as well as its ligand is necessary to further pursue this possibility.

Significance of Vesicle-Mediated E Release and Its Implication for Other Processes

The mechanism of steroid hormone transit through lipid membranes has not been well studied and in many physiology textbooks the issue is not even discussed. When this topic is mentioned, the explanation most often given is that they can freely diffuse through lipid membranes (Raven and Johnson, 2002; Sherwood, 2011; White and Porterfield, 2012). Despite this prevailing assumption, there are only a few reports where such transbilayer transfer of steroids by free diffusion has been analyzed. In one theoretical study, it was shown *in silico* that a free energy of solvation-based mechanism can produce rapid flux of estradiol, testosterone and progesterone through a simple membrane in concordance with measured rates (Oren et al., 2004). However, it is well known that steroid hormone transport across membranes can indeed be an active process in some situations: there are a number of reports on transporter involvement in either uptake or elimination of steroid hormones in eukaryotes ranging from yeast to human (Hock et al., 2000; Janvilisri et al., 2003; Kralli et al., 1995; Kralli and Yamamoto, 1996; Mahe et al., 1996). These reports are suggestive enough to rationalize a potential mechanism that incorporates steroid hormones into secretory vesicles, which enables regulated secretion of steroid hormones from steroidogenic tissues.

Historically, the possibility of vesicle-mediated steroid hormone release has been examined using ultrastructural and biochemical approaches in multiple biological systems, including the corpus luteum in sheep (Gemmell and Stacy, 1979; Gemmell et al., 1974; Higuchi et al., 1976; Sawyer et al., 1979). The proposed vesicle-mediated progesterone release from the sheep corpus luteum, however, was later challenged, since the peptide oxytocin was shown to be present in dense granules by immuno-EM methods (Theodosis et al., 1986) and release of oxytocin and progesterone responded differently to various secretagogues (Hirst et al., 1986). Since that time, studies investigating the possibility of vesicle-mediated steroid release in any biological system have rarely been reported. One relevant and intriguing set of studies, however, involved ultrastructural localization of E in the PG of the waxworm *Galleria mellonella* (Birkenbeil, 1983; Birkenbeil et al., 1979) using immuno-EM methods. These studies suggested that E in the PG is concentrated into what appear to be secretory granules that fuse with the plasma membrane, but once again no follow up studies have been reported in the literature.

In considering the various models for steroid passage through membranes, it is important to note that steroids such as progesterone, testosterone and estradiol are significantly more hydrophobic than E. Therefore, the free energy of solvation into a lipid bilayer of E is likely to be much more positive than for sex steroids; this may preclude the use of a simple diffusion mechanism for E. In this respect, E is more similar to bile acids, which are also highly hydrophilic and need active transporters to traverse lipid bilayers (Dawson et al., 2009). Thus, depending on their specific physiochemical properties, different steroids might use either simple passive diffusion through the plasma membrane, active transporters or some combination of these mechanisms.

In summary, our work provides strong evidence that E is released from the PG by calcium-stimulated, vesicle-mediated exocytosis. Therefore, we suggest that the prevailing “free diffusion” model of steroid hormone secretion needs to be reconsidered. It also follows that if E uses an active export process, then the import of many hormones, in particular 20E, is also likely controlled by transporters. Given the diversity of physiological processes regulated by steroid hormones, additional characterization of the mechanisms responsible for their import and export from various cell types and tissues will have significant impact on both basic and clinical aspects of steroid hormone physiology.

EXPERIMENTAL PROCEDURES

Fly Stocks

All flies were raised at 25°C on standard medium under 12 h/12 h light/dark cycle. Aside from the control strains of *yw* and *w*, transgenic flies used in the Figures are as follows: *phm22-Gal4* (Ou et al., 2011), *UAS-IP3R RNAi* (#6484, VDRC), *UAS-dicer2* (#60008 and #60009, VDRC), *UAS-Ras*^{V12} (#4847, BDSC), *UAS-CG34349 RNAi* (#31571, VDRC), *UAS-Rab3 RNAi* (100787, VDRC), *UAS-Syt1 RNAi* (#100608, VDRC), *UAS-GCaMP5* (#42038, BDSC), *UAS-gbb RNAi* (#5562R-1, NIG-FLY) *UAS-Gαq[Q203L]* (#30743, BDSC), *UAS-Syt-GFP* (#6926, BDSC), *UAS-Atet RNAi* (#42750, VDRC), *UAS-Sec10 RNAi* (a gift from K. Broadie; Andrews et al., 2002), *OK72-Gal4* (#6486, BDSC), *UAS-CG4822 RNAi* (#42730 and #105922, VDRC). All the other RNAi lines and sources used in this study are shown in Table 1. cDNA clones RE01860 and SD07027 from *Drosophila* Genomics Resource Center were used to tag *Atet* and *CG4822* with YPet or CyPet at N-termini using the recombineering-mediated method (Venken et al., 2008). These products were then cloned into pUAST and transgenic flies were generated by BestGene Inc (Chino Hills, CA).

Pupariation Timing and Developmental Arrest Phenotype Analyses

Synchronized newly hatched first instar larvae were placed on standard medium at 25°C, 25–30 larvae per vial, and pupariation timing of each individual was scored periodically. Developmentally arrested larvae were scored individually by checking their body and mouth hook characteristics. E feeding rescue was performed by adding 0.2 mg/ml (final concentration) of E into the medium. Larvae were transferred into E-free medium during the early third instar stage (80–104 h AEL) to avoid the potential detrimental effect of continuous E feeding.

Extraction of Ecdysteroids from CNS-RG Complexes and Hemolymph

Ten CNS-RG complexes were quickly dissected from larvae in PBS, briefly rinsed with PBS and pooled in 300 μl of methanol on ice. The complexes were thoroughly homogenized by repeatedly passing through 23 Gauge needles. After centrifugation at 4°C for 5 min, the supernatant was pooled on ice, while the pellet was re-extracted. The resulting extract (= 1 batch) was stored at −20°C until use. For hemolymph samples, 4 μl of hemolymph was collected from 10–20 larvae and mixed with 100 μl of methanol on ice. After vortexing, samples were centrifuged at 4°C for 5 min, and the resulting supernatant (=1 batch) was stored at −20°C until use.

Separation of E and 20E Using HPLC

For each HPLC experiment, 3 batches of CNS-RG extract or 1 batch of hemolymph sample was partially evaporated with a SpeedVac concentrator and diluted with water to make the methanol concentration 30% or lower. After centrifugation at room temperature for 10 min to remove precipitates, the aqueous solution was applied onto a Vydac 218TP C18 column (4.6 × 250 mm; Grace, Deerfield, IL) using Amersham Biosciences P-900 pump. The elution was performed with a linear gradient of 30–50% methanol over 20 min at the flow rate of 1 ml/min. The fractions were collected every 30 sec, and the amount of ecdysteroids in each fraction was determined by ecdysteroid ELISA using half the amount (250 μl) of each fraction. The residual half of each fraction corresponding to E (42.5–44.5% methanol = 1 ml) and 20E (36–38% methanol = 1 ml) were pooled and stored at -20°C until ecdysteroid quantification. This experiment was repeated 3 times for each biological sample.

Ecdysteroid ELISA

The sample solutions were dried with a SpeedVac concentrator and dissolved in EIA buffer (100 mM phosphate solution, pH 7.4, containing 0.1% BSA, 400 mM NaCl, 1 mM EDTA and 0.01% NaN_3). 20E AChE tracer (#482200), 20E EIA antiserum (#482202), Precoated (Mouse Anti-Rabbit IgG) EIA 96-Well Plates (#400007), and Ellman's Reagent (#400050) were all purchased from Cayman Chemical (Ann Arbor, MI). The assay was performed according to the manufacturer's instructions using synthetic E or 20E (Sigma-Aldrich, St. Louis, MO) as standards.

GCaMP5 Imaging and Data Analysis

Wandering third instar larvae were pinned down to a Sylgard dish and dissected in HL3 saline (2.5 mM Ca^{2+}) along the dorsal midline. All tissues with the exception of imaginal discs, CNS-RG complex and body wall musculature were removed. For the quantification of the PGs that presented calcium spikes (Figure 2F), the samples were treated with 1 μM tetrodotoxin in HL3 saline to block muscle contraction and stabilize the preparation. The samples were imaged in a Nikon FN1 microscope equipped with an A1R confocal scan head and a CFI75 Apo LWD 25× 1.1 NA water dipping objective. The PG was located using transmitted light and the zoom level was adjusted to include the whole PG within the field of view, which resulted in the pixel size of 0.25–0.33 μm. GCaMP5 was imaged with a 488 nm laser at constant power for all samples with the emission window of 500–550 nm. The experimental animals were coded so the imager didn't know the genotypes analyzed. The

time-lapse runs were analyzed for the presence of macro and micro spikes in calcium levels (GCaMP5 intensity) within the PG cells before decoding the genotypes. All image processing and analysis was performed with the Nikon NIS-Elements software package.

Fluorescence Microscopy

To avoid disruption of vesicle structures by sample fixation, the PGs were dissected and mounted in Schneider's insect medium (Sigma-Aldrich) and imaged immediately with fluorescence microscopy. All confocal images were acquired using a Zeiss LSM 710 (Carl Zeiss). A lambda scan was performed and the signals of Syt-GFP and YPet-Atet were linearly unmixed using ZEN 2009 software. For observation of the entire PG in Figures 3A and 3B, Zeiss Axio Imager M2 equipped with ApoTome.2 and Plan- Apochromat 20× 0.8 NA objective (Carl Zeiss) was used.

In Situ Hybridization

In situ hybridization with DIG-labeled RNA antisense probe was performed as previously described (Chavez et al., 2000). cDNA clones used to generate antisense probes are shown in Figure S3A.

Immunocytochemistry

cDNA clones RE01860 and RE53253 from *Drosophila* Genomics Resource Center were used, respectively, to generate HA-tagged Atet and E23 constructs. A nonsense mutation found in the E23 clone RE53253 (bp 2766) was corrected by site-directed mutagenesis (QuikChange Kit; Agilent Technologies, Santa Clara, CA) using following primers: 5'-GGCCCAGCACCTGGTGTGGTGTGCCGCGGACTCGCAGTCC-3'; 5'-GGACTGCGAGTCCGCGGCACACCACACCAGGTGCTGGGCC-3'. An *Xba*I site was introduced downstream of the start codon (Atet) or upstream of the stop codon (E23) and was used to insert a triple HA epitope. These products were then cloned into pBRAcpA expression vector for transient transfection into S2 cells (Rewitz et al., 2009). After transfection, cells were grown in serum-free M3 medium (Sigma-Aldrich) for 4 days and attached to concanavalin A-coated slides overnight at 25°C. Membrane permeabilization was performed with 0.1% Triton X-100 in PBS for 15 min at room temperature. Cells were stained with rat monoclonal anti-HA antibody 3F10 (1:500; Roche Applied Science, Indianapolis, IN) followed by Alexa Fluor 488 Goat Anti-Rat IgG antibody (1:1,000; Molecular Probes, Eugene, OR) pre-absorbed with S2 cells overnight at 4°C. Cells were briefly treated with PBS containing DAPI before mounted in Vectashield (Vector Laboratories, Burlingame, CA). Images were acquired using a Zeiss LSM 710 equipped with C-Apochromat 40× 1.2 NA water immersion and alpha Plan-Apochromat 100× 1.46 NA oil immersion objectives (Carl Zeiss).

Modified Vesicular Transport Assay

S2 cells were grown in 10-cm Petri dishes in serum-free M3 medium (Sigma-Aldrich) for 4 days after transfection with pBRAcpA empty vector (control), pBRAcpA-Atet or pBRAcpA-E23-HA. After pelleting by brief centrifugation at room temperature, the cells from two dishes were suspended in 4 ml ice-cold Extraction buffer (50 mM HEPES-KOH,

pH 7.5, containing 400 mM sucrose, supplemented with cOmplete, Mini, EDTA-free protease inhibitor cocktail, Roche Applied Science) and sonicated for 30 sec with a probe sonicator two times on ice. The cell lysates were then centrifuged at 1,000 × *g* for 5 min at 4°C to pellet cell debris, and the resultant supernatant was ultracentrifuged at 108,000 × *g* for 30 min at 4°C. The pellet (membrane fraction) was suspended in 1.6 ml Assay buffer (50 mM HEPES-KOH, pH 7.5, containing 10 mM $MgCl_2$) and sonicated for 30 sec with a probe sonicator on ice. The suspension was then immediately aliquoted (400 μl each) into four 1.5 ml tubes containing 50 μl E solution (100 μg/ml in Assay buffer) to incorporate E into vesicles. After 15 min, 50 μl of ATP solution (Sigma-Aldrich, 10 mM in Assay buffer) was added to each tube to give a final concentration of 1mM, and the transport assay was initiated. After 1 h incubation at 25°C, the vesicles were collected by filtrating through Whatman GF/A Glass microfiber filters (GE Healthcare). After washing three times with 1 ml 50 mM HEPES-KOH, pH 7.5, the filters were vigorously vortexed in 800 μl of methanol to extract E, and the E amount was determined by ecdysteroid ELISA.

Supplementary Material

Refer to Web version on PubMed Central for supplementary material.

ACKNOWLEDGEMENTS

We thank Vienna *Drosophila* Resource Center, Bloomington *Drosophila* Stock Center, NIG-FLY at National Institute of Genetics, Transgenic RNAi Project at Harvard Medical School and K. Broadie for fly stocks; *Drosophila* Genomics Resource Center for cDNA clones; members of O'Connor lab for fruitful discussion; and M.J. Shimell, A. Peterson, J. Simon and S. Conner for critical reading of the manuscript. GCaMP5 imaging and analysis was performed at the University Imaging Centers, University of Minnesota. This study was supported by a postdoctoral fellowship from the Japan Society for the Promotion of Science to N.Y., NIH grants K99/R00 HD073239 from NICHD to N.Y. and R01 GM093301 from NIGMS to M.B.O.

REFERENCES

Akerboom J, Chen TW, Wardill TJ, Tian L, Marvin JS, Mutlu S, Calderón NC, Esposti F, Borghuis BG, Sun XR, et al. Optimization of a GCaMP calcium indicator for neural activity imaging. J Neurosci. 2000; 32:13819–13840. [PubMed: 23035093]

Andrews HK, Zhang YQ, Trotta N, Broadie K. Drosophila sec10 is required for hormone secretion but not general exocytosis or neurotransmission. Traffic. 2002; 3:906–921. [PubMed: 12453153]

Aravamudan B, Fergestad T, Davis WS, Rodesch CK, Broadie K. Drosophila UNC-13 is essential for synaptic transmission. Nat Neurosci. 1999; 2:965–971. [PubMed: 10526334]

Birkenbeil H. Ultrastructural and immunocytochemical investigation of ecdysteroid secretion by the prothoracic gland of the waxmoth Galleria mellonella. Cell Tissue Res. 1983; 229:433–441. [PubMed: 6850754]

Birkenbeil H, Eckert M, Gersch M. Electron microscopical-immunocytochemical evidence of ecdysteroids in the prothoracic gland of Galleria mellonella. Cell Tissue Res. 1979; 200:285–290. [PubMed: 385145]

Caceres L, Necakov AS, Schwartz C, Kimber S, Roberts IJ, Krause HM. Nitric oxide coordinates metabolism, growth, and development via the nuclear receptor E75. Genes Dev. 2011; 25:1476–1485. [PubMed: 21715559]

Chapman ER. How does synaptotagmin trigger neurotransmitter release? Annu Rev Biochem. 2008; 77:615–641. [PubMed: 18275379]

Chavez VM, Marques G, Delbecque JP, Kobayashi K, Hollingsworth M, Burr J, Natzle JE, O'Connor MB. The Drosophila disembodied gene controls late embryonic morphogenesis and codes for a

cytochrome P450 enzyme that regulates embryonic ecdysone levels. Development. 2000; 127:4115–4126. [PubMed: 10976044]

Dawson PA, Lan T, Rao A. Bile acid transporters. J Lipid Res. 2009; 50:2340–2357. [PubMed: 19498215]

de Wit H, Walter AM, Milosevic I, Gulyas-Kovacs A, Riedel D, Sorensen JB, Verhage M. Synaptotagmin-1 docks secretory vesicles to syntaxin-1/SNAP-25 acceptor complexes. Cell. 2009; 138:935–946. [PubMed: 19716167]

Fukuda M. Regulation of secretory vesicle traffic by Rab small GTPases. Cell Mol Life Sci. 2008; 65:2801–2813. [PubMed: 18726178]

Gemmell RT, Stacy BD. Granule secretion by the luteal cell of the sheep: the fate of the granule membrane. Cell Tissue Res. 1979; 197:413–419. [PubMed: 572262]

Gemmell RT, Stacy BD, Thorburn GD. Ultrastructural study of secretory granules in the corpus luteum of the sheep during the estrous cycle. Biol Reprod. 1974; 11:447–462. [PubMed: 4477033]

Ghayee HK, Auchus RJ. Basic concepts and recent developments in human steroid hormone biosynthesis. Rev Endocr Metab Disord. 2007; 8:289–300. [PubMed: 17926129]

Graf ER, Valakh V, Wright CM, Wu C, Liu Z, Zhang YQ, DiAntonio A. RIM promotes calcium channel accumulation at active zones of the Drosophila neuromuscular junction. J Neurosci. 2012; 32:16586–16596. [PubMed: 23175814]

Higuchi T, Kaneko A, Abel JH Jr, Niswender GD. Relationship between membrane potential and progesterone release in ovine corpora lutea. Endocrinology. 1976; 99:1023–1032. [PubMed: 976187]

Hirst JJ, Rice GE, Jenkin G, Thorburn GD. Secretion of oxytocin and progesterone by ovine corpora lutea in vitro. Biol Reprod. 1986; 35:1106–1114. [PubMed: 3103698]

Hock T, Cottrill T, Keegan J, Garza D. The E23 early gene of Drosophila encodes an ecdysone-inducible ATP-binding cassette transporter capable of repressing ecdysone-mediated gene activation. Proc Natl Acad Sci U S A. 2000; 97:9519–9524. [PubMed: 10931948]

Huang X, Warren JT, Gilbert LI. New players in the regulation of ecdysone biosynthesis. J Genet Genomics. 2008; 35:1–10. [PubMed: 18222403]

Imai Y, Asada S, Tsukahara S, Ishikawa E, Tsuruo T, Sugimoto Y. Breast cancer resistance protein exports sulfated estrogens but not free estrogens. Mol Pharmacol. 2003; 64:610–618. [PubMed: 12920197]

Janvilisri T, Venter H, Shahi S, Reuter G, Balakrishnan L, van Veen HW. Sterol transport by the human breast cancer resistance protein (ABCG2) expressed in Lactococcus lactis. J Biol Chem. 2003; 278:20645–20651. [PubMed: 12668685]

Kall L, Krogh A, Sonnhammer EL. Advantages of combined transmembrane topology and signal peptide prediction--the Phobius web server. Nucleic Acids Res. 2007; 35:W429–W432. [PubMed: 17483518]

Kanno E, Fukuda M. Increased plasma membrane localization of O-glycosylation-deficient mutant of synaptotagmin I in PC12 cells. Journal of neuroscience research. 2008; 86:1036–1043. [PubMed: 18058942]

Klucken J, Buchler C, Orso E, Kaminski WE, Porsch-Ozcurumez M, Liebisch G, Kapinsky M, Diederich W, Drobnik W, Dean M, et al. ABCG1 (ABC8), the human homolog of the Drosophila white gene, is a regulator of macrophage cholesterol and phospholipid transport. Proc Natl Acad Sci U S A. 2000; 97:817–822. [PubMed: 10639163]

Kralli A, Bohen SP, Yamamoto KR. LEM1, an ATP-binding-cassette transporter, selectively modulates the biological potency of steroid hormones. Proc Natl Acad Sci U S A. 1995; 92:4701–4705. [PubMed: 7753868]

Kralli A, Yamamoto KR. An FK506-sensitive transporter selectively decreases intracellular levels and potency of steroid hormones. J Biol Chem. 1996; 271:17152–17156. [PubMed: 8663352]

Krogh A, Larsson B, von Heijne G, Sonnhammer EL. Predicting transmembrane protein topology with a hidden Markov model: application to complete genomes. J Mol Biol. 2001; 305:567–580. [PubMed: 11152613]

Kuwana H, Shimizu-Nishikawa K, Iwahana H, Yamamoto D. Molecular cloning and characterization of the ABC transporter expressed in Trachea (ATET) gene from Drosophila melanogaster. Biochim Biophys Acta. 1996; 1309:47–52. [PubMed: 8950175]

Langevin J, Morgan MJ, Sibarita JB, Aresta S, Murthy M, Schwarz T, Camonis J, Bellaiche Y. Drosophila exocyst components Sec5, Sec6, and Sec15 regulate DE-Cadherin trafficking from recycling endosomes to the plasma membrane. Dev Cell. 2005; 9:365–376. [PubMed: 16224820]

Li L, Chin LS. The molecular machinery of synaptic vesicle exocytosis. Cell Mol Life Sci. 2003; 60:942–960. [PubMed: 12827282]

Mahe Y, Lemoine Y, Kuchler K. The ATP binding cassette transporters Pdr5 and Snq2 of Saccharomyces cerevisiae can mediate transport of steroids in vivo. J Biol Chem. 1996; 271:25167–25172. [PubMed: 8810273]

Miller WL. Steroid hormone synthesis in mitochondria. Mol Cell Endocrinol. 2013; 379:62–73. [PubMed: 23628605]

Muller M, Liu KS, Sigrist SJ, Davis GW. RIM controls homeostatic plasticity through modulation of the readily-releasable vesicle pool. J Neurosci. 2012; 32:16574–16585. [PubMed: 23175813]

Murthy M, Garza D, Scheller RH, Schwarz TL. Mutations in the exocyst component Sec5 disrupt neuronal membrane traffic, but neurotransmitter release persists. Neuron. 2003; 37:433–447. [PubMed: 12575951]

Oren I, Fleishman SJ, Kessel A, Ben-Tal N. Free diffusion of steroid hormones across biomembranes: a simplex search with implicit solvent model calculations. Biophys J. 2004; 87:768–779. [PubMed: 15298886]

Ou Q, Magico A, King-Jones K. Nuclear Receptor DHR4 Controls the Timing of Steroid Hormone Pulses During Drosophila Development. PLoS Biol. 2011; 9:e1001160. [PubMed: 21980261]

Raven, PH.; Johnson, GB. Biology. Dubuque: MGraw-Hill; 2002. The Endocrine System; p. 1125-1146.

Rewitz KF, Yamanaka N, Gilbert LI, O'Connor MB. The insect neuropeptide PTTH activates receptor tyrosine kinase torso to initiate metamorphosis. Science. 2009; 326:1403–1405. [PubMed: 19965758]

Richmond JE, Broadie KS. The synaptic vesicle cycle: exocytosis and endocytosis in Drosophila and C. elegans. Curr Opin Neurobiol. 2002; 12:499–507. [PubMed: 12367628]

Richmond JE, Weimer RM, Jorgensen EM. An open form of syntaxin bypasses the requirement for UNC-13 in vesicle priming. Nature. 2001; 412:338–341. [PubMed: 11460165]

Rizo J, Rosenmund C. Synaptic vesicle fusion. Nat Struct Mol Biol. 2008; 15:665–674. [PubMed: 18618940]

Sapolsky RM, Romero LM, Munck AU. How do glucocorticoids influence stress responses? Integrating permissive, suppressive, stimulatory, and preparative actions. Endocr Rev. 2000; 21:55–89. [PubMed: 10696570]

Sawada K, Echigo N, Juge N, Miyaji T, Otsuka M, Omote H, Yamamoto A, Moriyama Y. Identification of a vesicular nucleotide transporter. Proc Natl Acad Sci U S A. 2008; 105:5683–5686. [PubMed: 18375752]

Sawyer HR, Abel JH Jr, McClellan MC, Schmitz M, Niswender GD. Secretory granules and progesterone secretion by ovine corpora lutea in vitro. Endocrinology. 1979; 104:476–486. [PubMed: 376288]

Sherwood, L. Fundamentals of Human Physiology. Belmont: Cengage Learning; 2011. Principles of Neural and Hormonal Communication; p. 71-105.

Shortridge RD, McKay RR. Invertebrate phosphatidylinositol-specific phospholipases C and their role in cell signaling. Invert Neurosci. 1995; 1:199–206. [PubMed: 9372143]

Sisk CL, Foster DL. The neural basis of puberty and adolescence. Nat Neurosci. 2004; 7:1040–1047. [PubMed: 15452575]

Sorrentino V, Barone V, Rossi D. Intracellular Ca(2+) release channels in evolution. Current opinion in genetics & development. 2000; 10:662–667. [PubMed: 11088018]

Sudhof TC. The synaptic vesicle cycle. Annu Rev Neurosci. 2004; 27:509–547. [PubMed: 15217342]

Sugita S, Han W, Butz S, Liu X, Fernandez-Chacon R, Lao Y, Sudhof TC. Synaptotagmin VII as a plasma membrane Ca(2+) sensor in exocytosis. Neuron. 2001; 30:459–473. [PubMed: 11395007]

Suzuki M, Suzuki H, Sugimoto Y, Sugiyama Y. ABCG2 transports sulfated conjugates of steroids and xenobiotics. J Biol Chem. 2003; 278:22644–22649. [PubMed: 12682043]

Talamillo A, Sanchez J, Cantera R, Perez C, Martin D, Caminero E, Barrio R. Smt3 is required for Drosophila melanogaster metamorphosis. Development. 2008; 135:1659–1668. [PubMed: 18367553]

Tarling EJ, Edwards PA. ATP binding cassette transporter G1 (ABCG1) is an intracellular sterol transporter. Proc Natl Acad Sci U S A. 2011; 108:19719–19724. [PubMed: 22095132]

Theodosis DT, Wooding FB, Sheldrick EL, Flint AP. Ultrastructural localisation of oxytocin and neurophysin in the ovine corpus luteum. Cell Tissue Res. 1986; 243:129–135. [PubMed: 2417717]

Tusnady GE, Simon I. The HMMTOP transmembrane topology prediction server. Bioinformatics. 2001; 17:849–850. [PubMed: 11590105]

Venkatesh K, Hasan G. Disruption of the IP3 receptor gene of Drosophila affects larval metamorphosis and ecdysone release. Curr Biol. 1997; 7:500–509. [PubMed: 9273145]

Venken KJ, Kasprowicz J, Kuenen S, Yan J, Hassan BA, Verstreken P. Recombineering-mediated tagging of Drosophila genomic constructs for in vivo localization and acute protein inactivation. Nucleic Acids Res. 2008; 36:e114. [PubMed: 18676454]

Wang N, Lan D, Chen W, Matsuura F, Tall AR. ATP-binding cassette transporters G1 and G4 mediate cellular cholesterol efflux to high-density lipoproteins. Proc Natl Acad Sci U S A. 2004; 101:9774–9779. [PubMed: 15210959]

Watanabe S, Tani T, Seno M. Transport of steroid hormones facilitated by serum proteins. Biochim Biophys Acta. 1991; 1073:275–284. [PubMed: 1826216]

White, BA.; Porterfield, SP. Endocrine and Reproductive Physiology. Maryland Heights: Mosby/Elsevier; 2012. Introduction to the Endocrine System; p. 1-25.

Yamanaka N, Rewitz KF, O'Connor MB. Ecdysone control of developmental transitions: lessons from Drosophila research. Annu Rev Entomol. 2013a; 58:497–516. [PubMed: 23072462]

Yamanaka N, Romero NM, Martin FA, Rewitz KF, Sun M, O'Connor MB, Leopold P. Neuroendocrine control of Drosophila larval light preference. Science. 2013b; 341:1113–1116. [PubMed: 24009394]

Yu L, Gupta S, Xu F, Liverman AD, Moschetta A, Mangelsdorf DJ, Repa JJ, Hobbs HH, Cohen JC. Expression of ABCG5 and ABCG8 is required for regulation of biliary cholesterol secretion. J Biol Chem. 2005; 280:8742–8747. [PubMed: 15611112]

Zhang YQ, Rodesch CK, Broadie K. Living synaptic vesicle marker: synaptotagmin-GFP. Genesis. 2002; 34:142–145. [PubMed: 12324970]

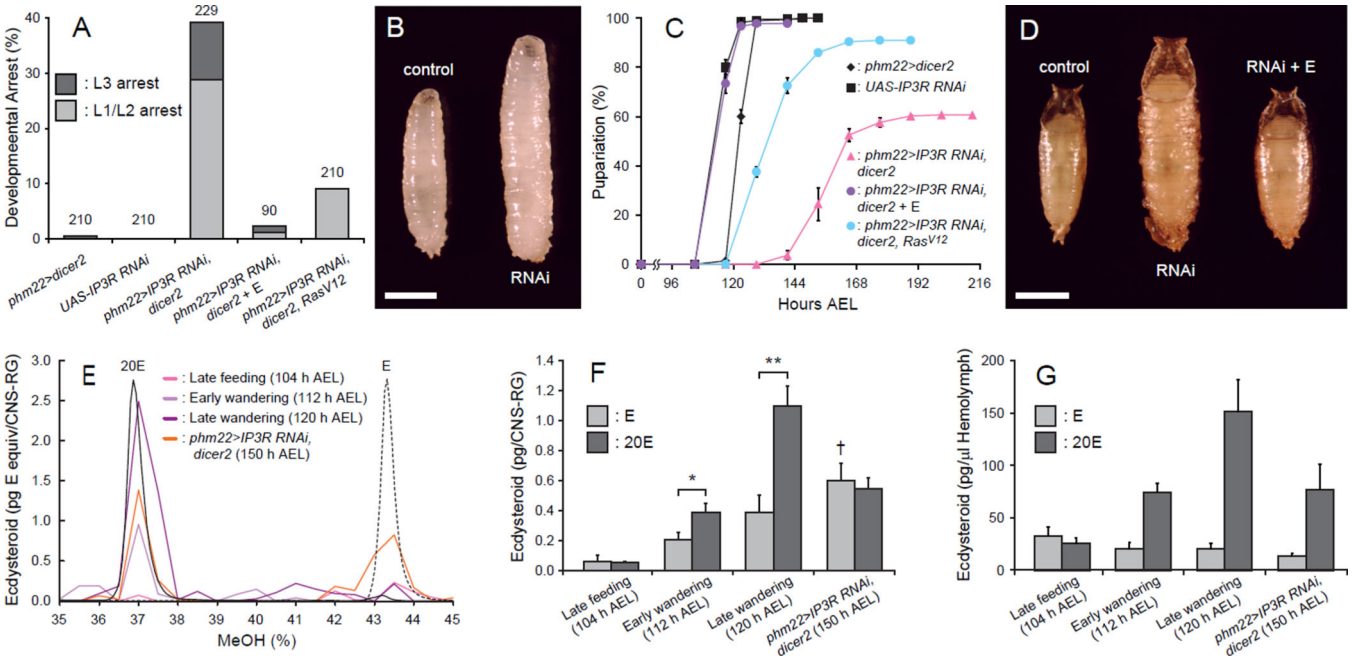

Figure 1. *IP3R* Is Required for E Secretion from the PG

(A) *IP3R*-knockdown in the PG causes polyphasic growth arrest. Percentages of developmentally arrested larvae for each genotype are shown. Percentages of larvae arrested at first or second instar (L1/L2) are indicated in light gray, whereas those arrested at third instar (L3) are shown in dark gray. E feeding is indicated by + E. Numbers of animals tested are shown on top of each bar.

(B) *IP3R*-knockdown in the PG causes overgrowth at L3. Representative image of a wandering control larva (control, *phm22>dicer2*) and an *IP3R*-knockdown larva arrested as L3 (RNAi, *phm22>IP3R RNAi, dicer2*). Scale bar, 1 mm.

(C) *IP3R*-knockdown in the PG causes developmental delay. Developmental time to pupariation of nonarrested larvae is shown. AEL, after egg laying. Data are represented as mean ± SEM of 3–7 independent experiments.

(D) *IP3R*-knockdown in the PG leads to the formation of overgrown pupae. Representative image of a control pupa (control, *phm22>dicer2*), an *IP3R*-knockdown pupa (RNAi, *phm22>IP3R RNAi, dicer2*) and an *IP3R*-knockdown pupa rescued by E feeding (RNAi + E, *phm22>IP3R RNAi, dicer2* with E feeding) is shown. Scale bar, 1 mm.

(E) Separation of E and 20E by a methanol (MeOH) gradient on reverse-phase HPLC. UV absorbance profiles at 248 nm of standard E (dashed black line) and 20E (solid black line) are shown on an arbitrary scale. The relative quantity of ecdysteroids in CNS-RG complexes of different groups of animals are shown in solid colored lines as E equivalent (pg) in each fraction. Fractions corresponding to 36–38% MeOH and 42.5–44.5% MeOH were pooled and used for 20E and E quantification, respectively.

(F) Quantity of ecdysteroids in CNS-RG complexes at different developmental times and larval genotypes. The E titer is indicated in light gray, whereas that of 20E is shown in dark gray. Each bar represents mean ± SEM of three independent sample preparations. *, $p<0.05$; **, $p<0.01$ from Student's t-test. †, $p<0.05$ compared to the amount of E in late feeding control larvae (ANOVA with Tukey's post-hoc test).

(G) Quantity of ecdysteroids in the hemolymph at different developmental times and larval genotypes. The E titer is indicated in light gray, whereas that of 20E is shown in dark gray. Each bar represents mean ± SEM of three independent sample preparations.

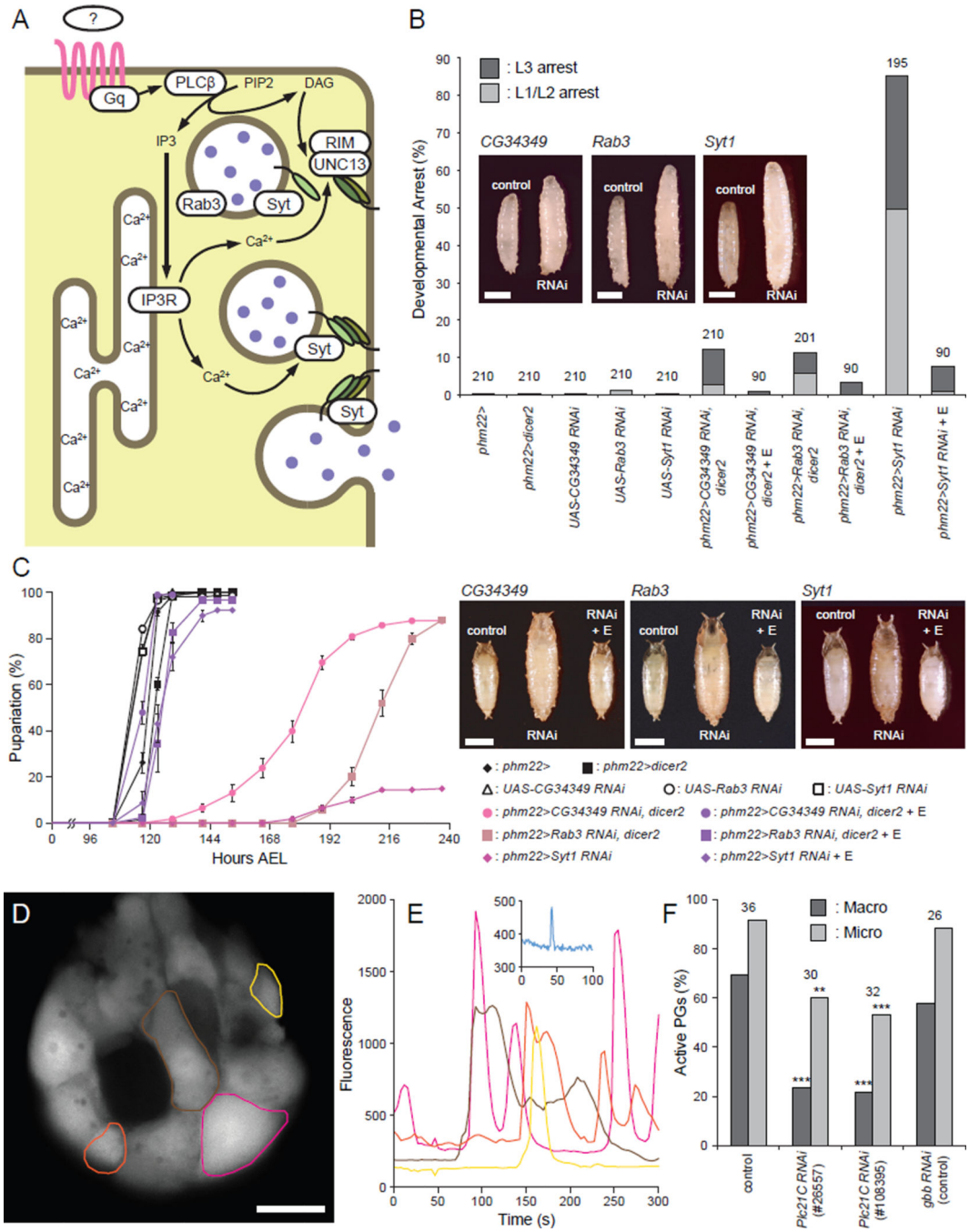

Figure 2. Regulatory Components of Secretory Vesicle Exocytosis Are Required in the PG for Normal Developmental Progression

(A) Schematic illustration of components involved in calcium-regulated vesicle exocytosis in the PG cells. An unknown GPCR is shown in pink, SNARE complex proteins are shown as green ovals, and E is depicted as purple filled circles.

(B) Knockdown of the regulatory components for secretory vesicle exocytosis in the PG causes polyphasic growth arrest. Percentages of developmentally arrested larvae for each genotype are shown. Percentages of larvae arrested at first or second instar (L1/L2) are indicated in light gray, whereas those arrested at third instar (L3) are shown in dark gray. E

feeding is indicated by + E. Numbers of animals tested are shown on top of each bar. Insets are representative images of wandering control larvae (control, *phm22>* or *phm22>dicer2*) and RNAi larvae arrested as L3 (RNAi). Scale bars, 1 mm.

(C) Knockdown of the regulatory components for secretory vesicle exocytosis in the PG causes developmental delay. Developmental time to pupation among non-arrested larvae is shown. Data are represented as mean ± SEM of 3–7 independent experiments. Insets are images of control pupae (control, *phm22>* or *phm22>dicer2*), RNAi pupae (RNAi) and RNAi pupae rescued by E feeding (RNAi + E). Scale bars, 1 mm.

(D) GCaMP5 calcium imaging of the PG cells from wandering third instar *phm22>GCaMP5* larvae. Cumulative maximum intensity projection of a 5-min time-lapse imaging is shown. Colored circles indicate the regions of interest (ROIs) where macro calcium spikes were observed. Scale bar, 25 μm.

(E) Plot of mean signal intensity in the cells indicated in (D). The color of each plot corresponds to that of the ROIs in (D). Inset is an example plot of a micro spike from a different sample.

(F) Quantification of the PGs that presented either macro (dark gray) or micro (light gray) calcium spikes in the animals of different genotypes (control, *phm22>GCaMP5*; RNAi, *phm22>GCaMP5, RNAi*). Numbers of animals observed are shown on top of each genotype. **, $p<0.01$; ***, $p<0.001$ from Fisher's exact test compared to control. See also Figure S2 and Movie S1.

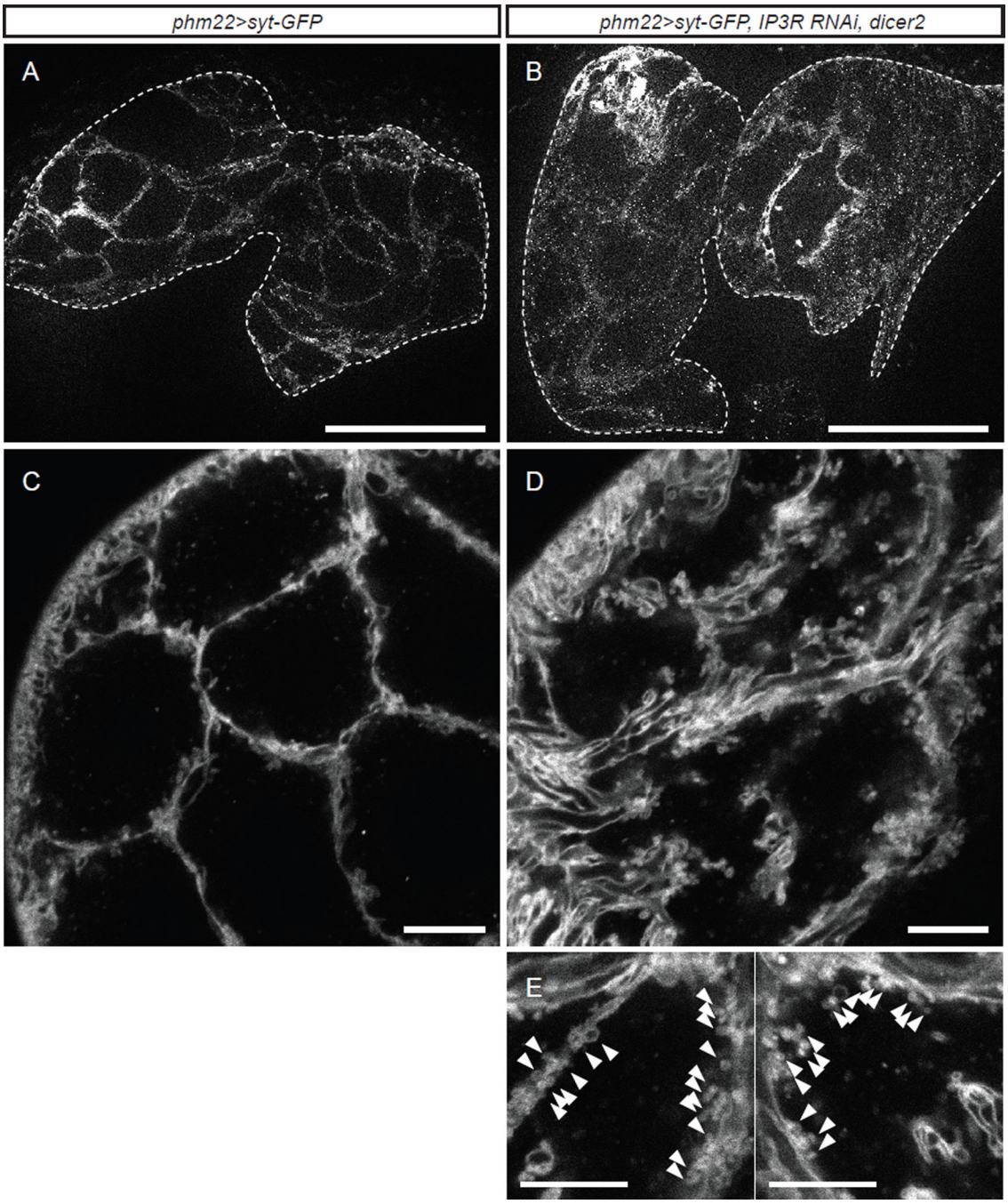

Figure 3. Syt-GFP Reveals the Presence of Vesicle-Like Structures in the PG

(A) Representative image of the PG from a wandering control larva overexpressing Syt-GFP (*phm22>Syt-GFP*). The PG is surrounded by a dashed line. Scale bar, 100 μm.

(B) Representative image of the PG from a day 7 (~150 h AEL) *IP3R* RNAi larva overexpressing Syt-GFP (*phm22>Syt-GFP, IP3R RNAi, dicer2*). The PG is surrounded by a dashed line. Scale bar, 100 μm.

(C) Confocal image of the PG from a wandering control larva overexpressing Syt-GFP. Scale bar, 10 μm.

(D) Confocal image of the PG from a day 7 (~150 h AEL) *IP3R* RNAi larva overexpressing Syt-GFP. Scale bar, 10 μm.

(E) Magnified view of the PG cells from day7 (~150 h AEL) *IP3R* RNAi larvae overexpressing Syt-GPF. Note aggregation of many small vesicle-like structures along the membrane (arrowheads). Scale bars, 10 μm.

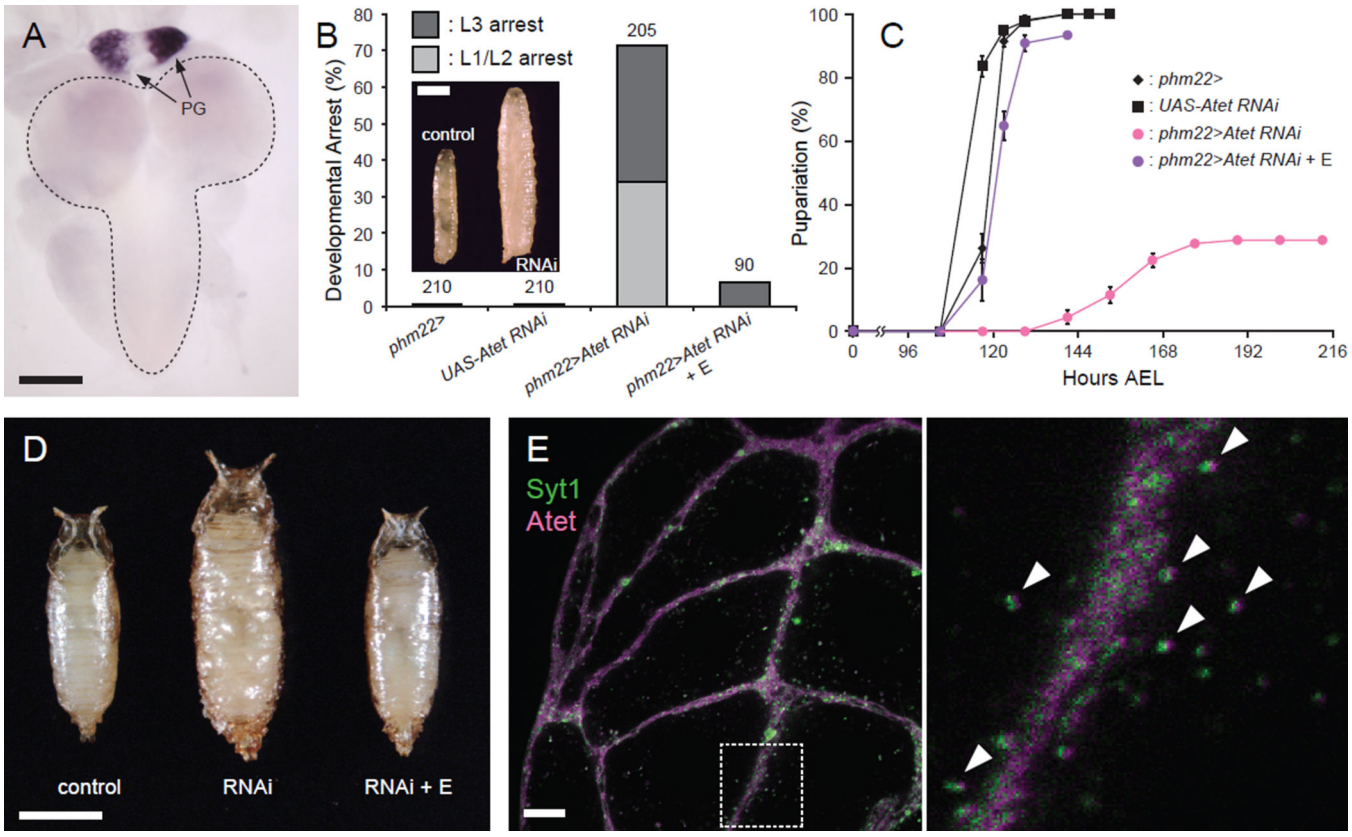

Figure 4. *Atet* Is Expressed in the PG and Required for Normal Developmental Progression

(A) *Atet* is highly expressed in the PG, as shown by *in situ* hybridization of the CNS-RG complex from a wandering larva with an *Atet* antisense probe. The PG components of the RG are indicated by arrows, and the CNS is surrounded by a dashed line. Scale bar, 100 μm.

(B) *Atet*-knockdown in the PG causes polyphasic growth arrest. Percentages of developmentally arrested larvae for each genotype are shown. Percentages of larvae arrested at first or second instar (L1/L2) are indicated in light gray, whereas those arrested at third instar (L3) are shown in dark gray. E feeding is indicated by + E. Numbers of animals tested are shown on top of each bar. Inset is a representative image of a wandering control larva (control, *phm22>*) and an *Atet* RNAi larvae arrested as L3 (RNAi, *phm22>Atet RNAi*). Scale bar, 1 mm.

(C) *Atet*-knockdown in the PG causes developmental delay. Developmental time to pupation among nonarrested larvae is shown. Data are represented as mean ± SEM of 3–7 independent experiments.

(D) *Atet*-knockdown in the PG leads to the formation of overgrown pupae. Representative image of a control pupa (control; *phm22>*), an *Atet*-knockdown pupa (RNAi, *phm22>Atet RNAi*) and an *Atet*-knockdown pupa rescued by E feeding (RNAi + E, *phm22>Atet RNAi* with E feeding). Scale bar, 1 mm.

(E) Syt1 and Atet co-localize in the PG. Representative confocal image of the PG from a wandering larva overexpressing Syt-GFP (green) and YPet-Atet (magenta). The square area surrounded by a dashed line in the left panel is magnified on the right. Vesicles labeled by

both Syt-GFP and YPet-Atet are indicated by arrowheads. Scale bar, 10 μm. See also Figure S3.

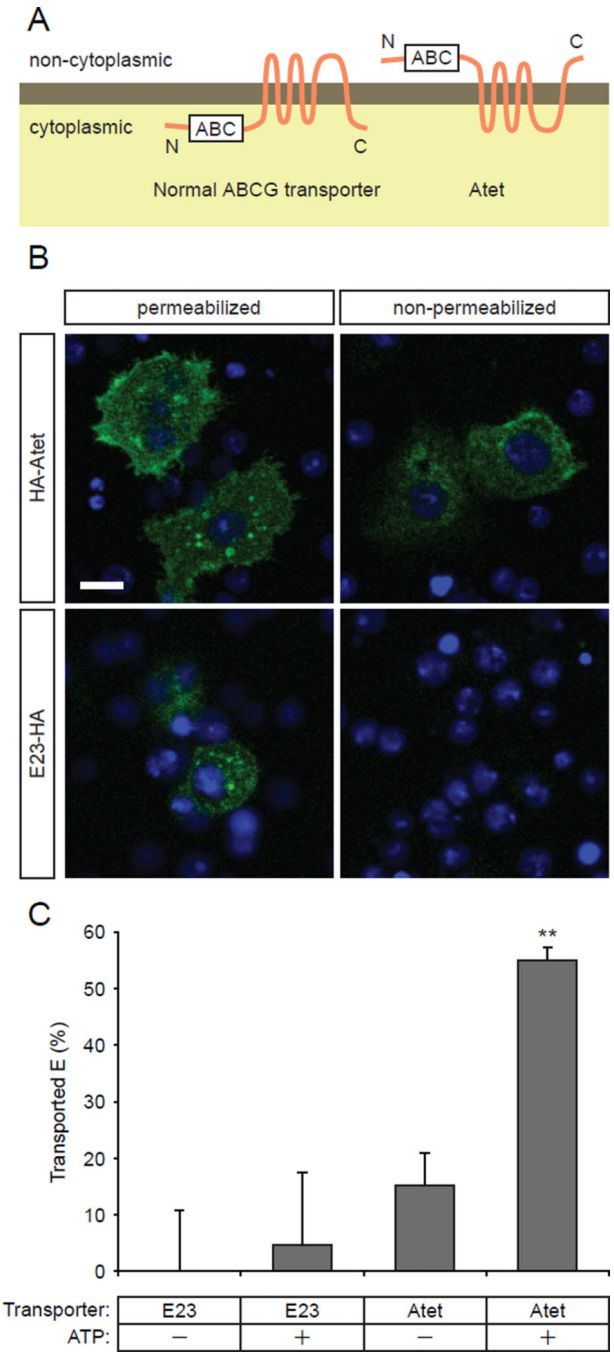

Figure 5. Atet Is An E Transporter

(A) Membrane topology of a normal ABC-type transporter (left) and of Atet (right) as predicted by membrane topology prediction servers. White boxes indicate the ATP bind cassette (ABC).

(B) Anti-HA staining of S2 cells overexpressing N-terminally-tagged Atet (HA-Atet) or C-terminally-tagged E23 (E23-HA) in permeabilized and non-permeabilized conditions. The C-terminus of E23 was consistently predicted by prediction servers (Phobius, TMHMM and HMMTOP) to be intracellular and therefore used as a negative control.

(C) E transporting activity of Atet and E23 measured by modified vesicular transport assay. Data are represented as mean ± SEM of 5–6 independent experiments. **, $p<0.01$ compared to control (0% transport) from Student's t-test. See also Figure S4 for the details of the modified vesicular transport assay.

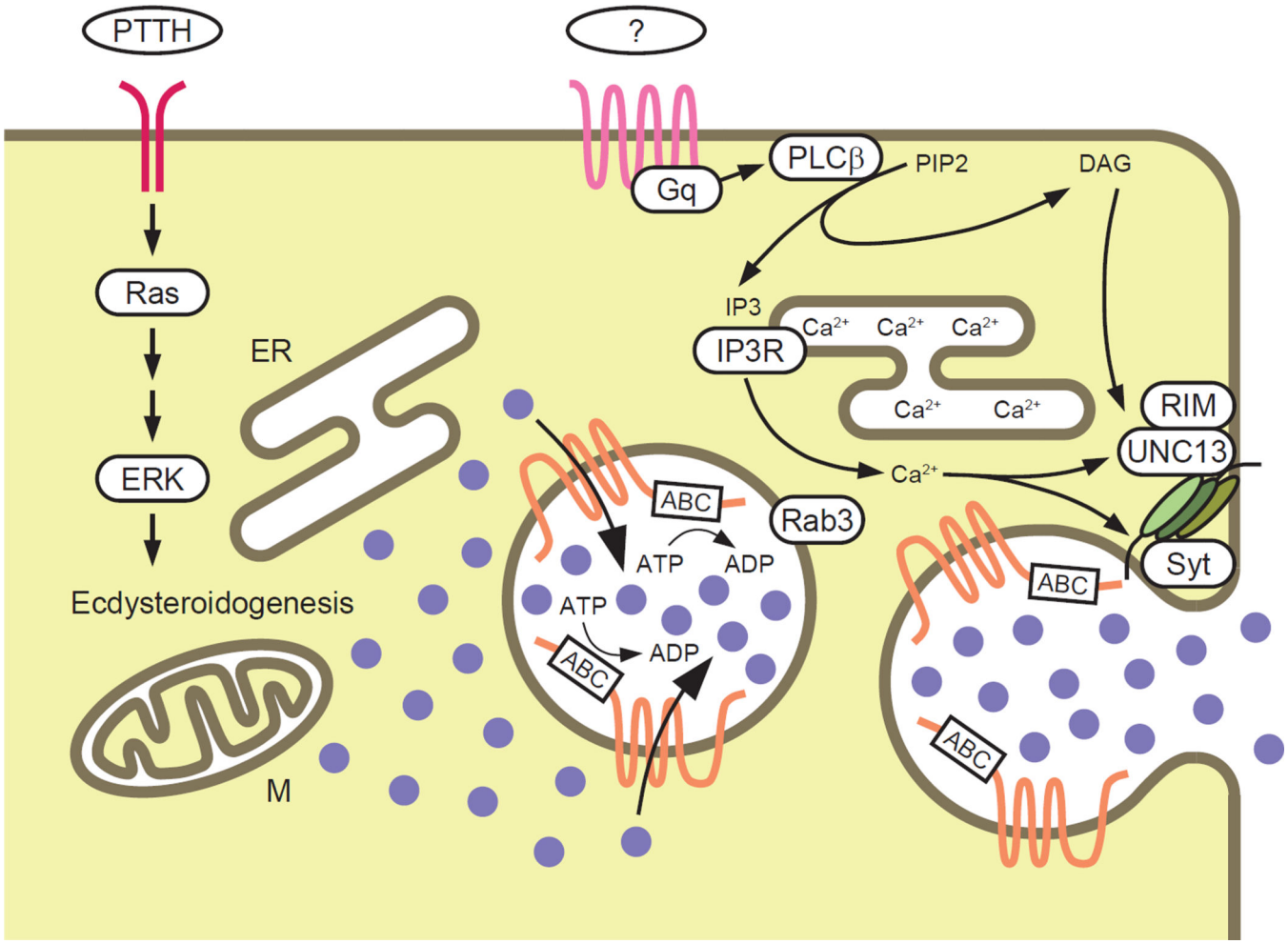

Figure 6. Schematic Illustration of the Vesicle-Mediated E Release Model

Torso is shown in red, an unknown GPCR is shown in pink, and Atet is shown in orange. E is depicted as purple filled circles. ER, endoplasmic reticulum; M, mitochondria.

Table 1

RNAi Screening of Genes Involved in Membrane Traffic, Intracellular Calcium Signaling or Regulated Vesicle Exocytosis

	Classification	Gene Name	CG Number	VDRC Transformant ID	Phenotype
Membrane traffic	Synaptobrevin	*Syb*	CG12210	**39770, 102922**	**Developmental Delay/Arrest**
		n-Syb	CG17248	44011, 49201, 104531	No
	Exocyst	*Sec3*	CG3885	35806, 108085	No
		Sec5	CG8843	**28873**	**Developmental Delay/Arrest**
		Sec6	CG5341	**22077, 105836**	**Developmental Delay/Arrest**
		Sec8	CG2095	**45032, 105653**	**Developmental Delay/Arrest**
		Sec10	CG6159	**N/A***	**Developmental Delay/Arrest**
		Sec15	CG7034	**35161, 105126**	**Developmental Delay/Arrest**
		exo70	CG7127	27867, 103717	No
		exo84	CG6095	**30111, 108650**	**Developmental Delay/Arrest**
Intracellular Ca^{2+} release	Gαq	*CG30054*	CG30054	**4643**†, **4644**, 102887	**Developmental Delay/Arrest**
		Gαq	CG17759	50729, 105300	No
		CG17760	CG17760	42255, 52308, 107613	No
	Phospholipase C	*Plc21C*	CG4574	**26557, 108395**†	**Developmental Delay/Arrest**
		norpA	CG3620	105676	No
		PLCγ	CG4200	7173, 108593	No
	ER Ca^{2+} Channel	*IP3R*	CG1063	**6484**†, 106982	**Developmental Delay/Arrest**
		RyR	CG10844	109631	No
Ca^{2+}-regulated exocytosis	UNC-13	*CG34349*	CG34349	**31571**†, **31573**, 107855	**Developmental Delay/Arrest**
		UNC-13	CG2999	33606, 33609, 101383	No
		UNC-13-4A	CG32381	41835, 109304	No
	Secretory Rab	*Rab3*	CG7576	**100787**†	**Developmental Delay/Arrest**
		Rab26	CG34410	43730, 101330	No
		Rab27	CG14791	31887**, 35774**	No
	RIM	*RIM*	CG33547	**48072**†, 39384	**Developmental Delay/Arrest**

	Classification	Gene Name	CG Number	VDRC Transformant ID	Phenotype
	Synaptotagmin	*Syt1*	CG3139	**100608**[†], 8874	**Developmental Delay/Arrest**
		Syt4	CG10047	33317	No
		Syt7	CG2381	24988	No
		Syt12	CG10617	47504, 47506, 110655	No
		Syt14	CG9778	11037	No
		*Sty*α	CG5559	9303, 100957	No
		*Syt*β	CG42333	30013, 103345	No

UAS-RNAi lines from Vienna Drosophila RNAi Center (VDRC) were crossed to *phm22>dicer2* to induce tissue-specific knockdown in the PG. Lines that exhibited the developmental delay/arrest phenotype are shown in bold. Multiple RNAi lines were tested for each gene whenever available to minimize the false-positive results from off-target effects.

[*], kind gift from K. Broadie;

[**], lines from Transgenic RNAi Project at Harvard Medical School (obtained from Bloomington Drosophila Stock Center).

[†], phenotypic rescue with E feeding was confirmed.

See also Figure S1.